A numerically stable magnetic anomaly formula for uniform polyhedra

Horst Holstein, Aberystwyth University & Intrepid Geophysics, and Costas Anastasiades, Aberystwyth University*

SUMMARY

Standard gravi-magnetic anomaly formulae for uniform polyhedral targets require summation of terms that can, with increasing target distance, far exceed their resultant sum. In the context of floating point arithmetic such formulae become numerically unstable on account of destructive cancellation during summation. This limits the usability of the formulae to a maximum target range. Recent work has shown how the instability may be overcome in the case of thin polygonal targets. The close formulation between polygonal sheet and polyhedral target anomaly formulae allows us to generalize stabilization to the polyhedral case. We derive a stabilized polyhedral magnetic anomaly formula, and demonstrate its zero error growth with increasing target distance. Stability is achieved at the cost of some extra numerical complexity. The approach can be extended to all the polyhedral gravi-magnetic anomaly formulae.

INTRODUCTION

Floating point arithmetic with finite precision ε induces a well documented numerical instability in the standard anomaly formulae for uniform polyhedral targets (Strakhov et al. (1986), Holstein et al. (1999)). Beyond a certain target distance, numerical evaluation of the formulae fails to produce any correct significant digits, due to destructive cancellation in summing oppositely signed terms that are large compared to the final correct result.

The large summands originate from the analytical point source integral over the target volume to obtain a closed form solution. The integration is performed in three stages: volume to surface, surface to line, and line to vertex (end-point). For example, with constant of universal gravitation G and density ρ, volume to surface integration leads to

$$G\rho \int_V \nabla\left(\frac{1}{r}\right) dV \;=\; G\rho \sum_i \mathbf{n}_i \int_{S_i} \frac{dS}{r}\;. \qquad (1)$$

where $\mathbf{n}_i$ is the unit outward normal to facet i of the polyhedron. Setting $\gamma = \alpha/\delta$, where α is a typical target dimension and δ is a typical distance of the target from the observation point, the left hand integral in equation (1) is seen to be of $O(\alpha^3/\delta^2) = O(\alpha\gamma^2)$, while the right hand side is a sum of terms of $O(\alpha^2/\delta) = O(\alpha\gamma)$. This represents a growth of γ^{-1}, becoming unbounded as the target distance increases. The remaining two integration stages each introduce a further factor γ, so that the final analytical anomaly expression is a sum of terms $O(\gamma^{-3})$ larger than the sum itself. This is the cause of the numerical instability during floating point evaluation.

The right hand side of equation (1) may be interpreted as a vector sum of potentials from polygonal sheets represented by the polyhedral facets. This indicates that the anomaly formula for a thin polygonal sheet is related to the gradient of that anomaly for a polyhedral target. Significantly, the anomaly formula for a thin sheet requires only two integration stages (surface to line, line to vertex), and hence its summands suffer only two magnification steps, or γ^{-2}. Error growth is therefore less rapid in the sheet model.

Stabilization will be achieved by cancellation of dominant terms prior to numerical evaluation. Successive reduction of two of the growth terms in polyhedral formulae was achieved by Holstein et al. (1999). Realization that this approach could eliminate the two growth factors in the sheet anomalies to achieve stabilized zero-error growth sheet formulae came in Holstein and Anastasiades (2010a,b). It is the purpose of this article to extend the sheet results to also achieve stabilized polyhedral anomaly formulae. We demonstrate this for the magnetic field polyhedral anomaly formula.

TARGET GEOMETRY

Consider a polygonal sheet, or equivalently, a polygonal facet of a polyhedral target. Let its (outward) unit normal be $\mathbf{n}$, and its edges be enumerated by subscript j. Let edge j have a unit tangent vector $\mathbf{t}_j$ oriented counter clockwise around $\mathbf{n}$, and an in-plane outward unit vector $\mathbf{h}_j$ perpendicular to edge and normal, as shown in Figure 1. Relative to a local target origin,

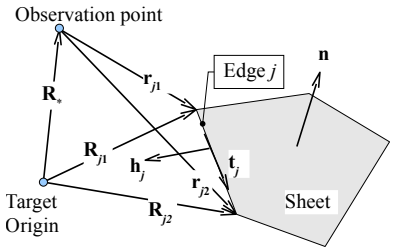

Figure 1: Reference systems for a sheet target or a facet.

the position vectors of edge j vertices $\mathbf{R}_{j1}$, $\mathbf{R}_{j2}$ are ordered anticlockwise around facet normal $\mathbf{n}$. The position vector of the observation point is $\mathbf{R}_*$. Relative to the observation point, position vectors to the target vertices are

$$\mathbf{r}_{j1} = \mathbf{R}_{j1} - \mathbf{R}_*\;,\;\; \mathbf{r}_{j2} = \mathbf{R}_{j2} - \mathbf{R}_*\;. \qquad (2)$$

Vertex vector projections, edge lengths, mid-points and magnitudes are defined by

$$\begin{aligned} h_j &= \mathbf{h}_j \bullet \mathbf{r}_{jk},\; \ell_{jk} = \mathbf{t}_j \bullet \mathbf{r}_{jk}, r_{jk} = \left|\mathbf{r}_{jk}\right|, k = 1,2, \\ \mathscr{L}_j &= \left|\mathbf{R}_{j2} - \mathbf{R}_{j1}\right|,\; \bar{\mathbf{R}}_j = \tfrac{1}{2}(\mathbf{R}_{j1} + \mathbf{R}_{j2}), \\ \bar{\mathbf{r}}_j &= \tfrac{1}{2}(\mathbf{r}_{j1} + \mathbf{r}_{j2}),\; \bar{r}_j = \tfrac{1}{2}(r_{j1} + r_{j2}) \\ v &= \bar{\mathbf{r}}_j \bullet \mathbf{n}, j = 1,2,\ldots\;. \end{aligned} \qquad (3)$$

We assume that the local target origin is $O(\alpha)$ from any vertex. Crucially, the difference $\left|\mathbf{r}_{j2}-\mathbf{r}_{j1}\right|$ of $O(\delta)$ vectors can now be computed as the $O(\alpha)$ edge length $\mathscr{L}_j$, as above.

GOVERNING EQUATIONS AND REVIEW

Integration of equation (1), and the use of Poisson's relation, gives the sheet potential φ and the polyhedral field $\mathbf{f}$, subscripted by g and m for gravity and magnetic cases, as

$$\begin{aligned}\varphi_g &= -G\rho\sum_j \mathbf{b}_j\bullet\bar{\mathbf{r}}_j\ , \quad \mathbf{f}_g = G\rho\sum_i \mathbf{n}_i\sum_j \mathbf{b}_{ij}\bullet\bar{\mathbf{r}}_{ij}\\ \varphi_m &= -T\mathbf{m}\bullet\sum_j \mathbf{b}_j\ , \quad \mathbf{f}_m = \mathbf{m}\bullet\sum_i \mathbf{n}_i\sum_j \mathbf{b}_{ij}\end{aligned} \tag{4}$$

where $\mathbf{m}$ is the magnetization vector and T is the thickness of the sheet (Holstein et al. (2009)). The subscript i in the polyhedral formulae indicates facet enumeration.

Direct integration expresses $\mathbf{b}_j$, omitting facet subscript i, as

$$\mathbf{b}_j = \left[\mathbf{h}_j \ln\frac{r_{jk}+\ell_{jk}}{\bar{r}_j} - \tilde{\mathbf{n}}\left\{\arctan\frac{\ell_{jk}}{h_j} - \arctan\frac{|v|\ell_{jk}}{r_{jk}h_j}\right\}\right]_{k=1}^{k=2} \tag{5}$$

with $\tilde{\mathbf{n}} = \text{sign}(v)\mathbf{n}$. We call this the "vertex method", as differencing occurs over the vertex end points of each facet edge.

Analytical differencing, to eliminate one growth factor, leads to the "line method" formula of Strakhov et al. (1986),

$$\mathbf{b}_j = 2\mathbf{h}_j\text{arctahn}\Lambda_j - 2\tilde{\mathbf{n}}\arctan\lambda_j \tag{6}$$

where

$$\Lambda_j = \frac{\mathscr{L}_j}{2\bar{r}_j},\ \ \lambda_j = \frac{h_j\Lambda_j}{\tilde{r}_j},\ \ \tilde{r}_j = \bar{r}_j(1-\Lambda_j^2)+|v|\ . \tag{7}$$

with consequent reduction in the summands $\mathbf{b}_j$ from $O(1)$ in formulae (5) to $O(\gamma)$ in formula (6).

Holstein (2002) induced a second $O(\gamma)$ reduction by constructing offsets $\mathbf{b}_j^*$ that allow dominant term removal in $\delta\mathbf{b}_j = (\mathbf{b}_j - \mathbf{b}_j^*)$, while accumulating offsets $\sum_j \mathbf{b}_j^*$ as a pyramidal vector area, vertexed at the observation point, that collapses to the facet base area, smaller by a factor $O(\gamma)$, according to

$$\sum_j \mathbf{b}_j \ = \ \sum_j \delta\mathbf{b}_j \ + \ \sum_j \mathbf{b}_j^*\ . \tag{8}$$

To this end, first introduce the facet centroid at position $\mathbf{R}_c$ relative to the local target origin, and position $\mathbf{r}_c$ (magnitude r_c) relative to the observation point (see Figure 1), and then recast equations (6) and (7) in terms of centroid related quantities

$$\mathbf{b}_j^* = 2\mathbf{h}_j\Lambda_j^* - 2\tilde{\mathbf{n}}\lambda_j^*, \tag{9}$$

$$\Lambda_j^* = \frac{\mathscr{L}_j}{2r_c},\ \ \lambda_j^* = \frac{h_j\Lambda_j}{\tilde{r}_c},\ \ \tilde{r}_c = r_c+|v|\ . \tag{10}$$

As $\gamma\to 0$ with increasing target distance, the differences

$$\begin{aligned}\delta\Lambda_j &= \Lambda_j - \Lambda_j^* = O(\gamma^2),\\ \delta\lambda_j &= \lambda_j - \lambda_j^* = O(\gamma^2),\\ \text{Atnh}(\Lambda_j) &= (\text{arctanh}(\Lambda_j)-\Lambda_j)/\Lambda_j^3 = O(1),\\ \text{Atn}(\lambda_j) &= (\arctan(\lambda_j)-\lambda_j)/\lambda_j^3 = O(1)\end{aligned} \tag{11}$$

must be computed from the formulae in Appendix A that have achieved dominant term removal, to avoid numerical destructive cancellation. The resulting "surface method" achieves a reduction of terms by a factor $O(\gamma^2)$ over the vertex method (5), and is summarized by equations (8) and

$$\delta\mathbf{b}_j \ = \ 2\mathbf{h}_j(\Lambda_j^3\text{Atnh}\,\Lambda_j + \delta\Lambda_j) - 2\tilde{\mathbf{n}}(\lambda_j^3\text{Atn}\,\lambda_j + \delta\lambda_j) \tag{12}$$

$$\sum_j \mathbf{b}_j^* = \ -2\tilde{\mathbf{n}}A/(r_c\tilde{r}_c) \tag{13}$$

where A is the area of the facet.

We noted above that sheet anomaly formulae suffer only two growth factors. Since the surface method removes two such factors, Holstein and Anastasiades (2010a) argued that sheet surface method anomaly formulae should be stable with zero error growth, and verified this to be the case. By contrast, polyhedral surface anomaly formulae retain one error growth factor, and so remain numerically moderately unstable.

A NEW STABLE POLYHEDRAL MAGNETIC ANOMALY FORMULA: THE VOLUME METHOD

In this section we explore how insights from the sheet anomaly formulae can be used to remove the final growth factor in the polyhedra anomaly formula, to produce a stable zero error growth anomaly formula. We call such a formula a "volume method", as cancellation of the last factor can only be brought about by considering all the polyhedral facets that enclose the target volume. The terms generated in the volume formula will be of the order of the integrand in the volume integral for the anomaly. Hence no destructive cancellation will take place on numerical evaluation.

From equations (12) and (13), the dominant $O(\gamma^2)$ terms arising during of equation (8) are

$$\sum_j \left(2\mathbf{h}_j\delta\Lambda_j - 2\tilde{\mathbf{n}}\delta\lambda_j\right) - 2\tilde{\mathbf{n}}A/(r_c\tilde{r}_c)\ . \tag{14}$$

Holstein and Anastasiades (2010b) argued that this must contain the dominant equivalent point source term, namely $-A\mathbf{r}_c/r_c^3$. This fact is hidden, because $\delta\Lambda_j$ and $\delta\lambda_j$ still retain dependence on r_{j1} and r_{j2}. We therefore replace them by r_c in newly introduce terms $\delta\Lambda_j^*, \delta\lambda_j^*$, and define stabilized differences

$$\delta^2\Lambda_j = \delta\Lambda_j - \delta\Lambda_j^*,\ \ \delta^2\lambda_j = \delta\lambda_j - \delta\lambda_j^*\ , \tag{15}$$

by cancelling the dominant $O(\gamma^2)$ terms to yield results of $O(\gamma^3)$, as in Appendix B. The second order terms in equation (14) now combine into the point source term

$$-A\mathbf{r}_c/r_c^3 = -2A\tilde{\mathbf{n}}/(r_c\tilde{r}_c) + \sum_j\left(2\mathbf{h}_j\delta\Lambda_j^* - 2\tilde{\mathbf{n}}\delta\lambda_j^*\right) \tag{16}$$

leading to a modified surface method (8)

$$\sum_j \mathbf{b}_j = \sum_j \delta\mathbf{b}_j^* \ - \ A\mathbf{r}_c/r_c^3 \tag{17}$$

$$\delta\mathbf{b}_j^* = 2\mathbf{h}_j(\Lambda_j^3\text{Atnh}\Lambda_j + \delta^2\Lambda_j) - 2\tilde{\mathbf{n}}(\lambda_j^3\text{Atn}\lambda_j + \delta^2\lambda_j)\ . \tag{18}$$

The significance of this form is that the dominant $O(\gamma^2)$ terms are captured entirely by the point source term, with higher terms of $O(\gamma^3)$ contained in the $\delta\mathbf{b}_j^*$ terms as a manifestation of the finite sheet geometry.

Following (4), we now regard the polyhedral anomaly $\mathbf{f}_m$ as a sum of sheet contributions. All terms in equations (17) and (18) therefore bear an extra initial subscript i, enumerating the facets.

The centroid of sheet i will now be at position vector $\mathbf{r}_{ic}$ relative to the observation point, with magnitude r_{ic}. Relative to the local target origin, the position vector is $\mathbf{R}_{ic}$. We take the centroid of the whole polyhedral target to be at $\mathbf{r}_p$ relative to the observation point, and $\mathbf{R}_p$ relative to the target origin. The displacement $(\mathbf{r}_{ic}-\mathbf{r}_p)$ from the target centroid to facet centroid is a difference of $O(\delta)$ vectors, but equals the difference $(\mathbf{R}_{ic}-\mathbf{R}_p)$ of $O(\alpha)$ vectors, irrespective of the location of the observation point. This allows the Newtonian response $\mathbf{r}_{ic}/r_{ic}^3$ of facet i to be expressed as a response from the target centroid plus an $O(\gamma/\delta^2)$ offset $<\mathbf{r}_{ic},\mathbf{r}_p>$ that can be calculated (eq.(C-1)) without destructive cancellation

$$\mathbf{r}_{ic}/r_{ic}^3 = \mathbf{r}_p/r_p^3 + <\mathbf{r}_{ic},\mathbf{r}_p> \ . \qquad (19)$$

Substitution of equation (17) into equation (4) to obtain $\mathbf{f}_m$ will require the summation

$$\sum_i \mathbf{n}_i A_i \mathbf{r}_{ic}/r_{ic}^3 = \sum_i \mathbf{n}_i A_i (\mathbf{r}_p/r_p^3 + <\mathbf{r}_{ic},\mathbf{r}_p>) \ . \qquad (20)$$

Closure of the polyhedral target ensures that the sum of its vector facet areas is zero, causing the remaining highest order $O(\gamma^2)$ terms to collapse to zero. This leads to the final result

$$\mathbf{f}_m = \mathbf{m}\bullet \sum_i \mathbf{n}_i \sum_j (\delta\mathbf{b}_{ij}^* + A_i <\mathbf{r}_{ic},\mathbf{r}_p>) \ , \qquad (21)$$

with $O(\gamma^3)$ summands. The three growth terms in the vertex method have been removed in the new volume method, and this will be reflected in the error plots.

RESULTS

As reference anomaly solution, we used a point source of magnetization $V\mathbf{m}$, where V is the volume of a polyhedral test target and $\mathbf{m}$ is its magnetization per unit volume. The point source formula has no destructive cancellation, and can be used at any target distance. With increasing target distance, we expect the polyhedral anomaly to approach that of the point source, until further closeness is prevented by the finite precision. As measure of the relative closeness of the polyhedral and points source magnetic anomalies $\mathbf{a}_{poly}$ and $\mathbf{a}_{point}$ respectively, we use a relative error measure

$$\text{relative difference} = \max\left\{\frac{||\mathbf{a}_{poly}-\mathbf{a}_{point}||}{||\mathbf{a}_{point}||}, \varepsilon\right\} \ . \qquad (22)$$

Here $\varepsilon \approx 10^{-15.7}$ is the machine floating point precision constant, and provides the correct lower bound for the relative difference of two nearly equal floating point numbers. The logarithm of the relative difference is then always defined. As test target, we took a triangular prismatic polyhedron shown in Figure 2.

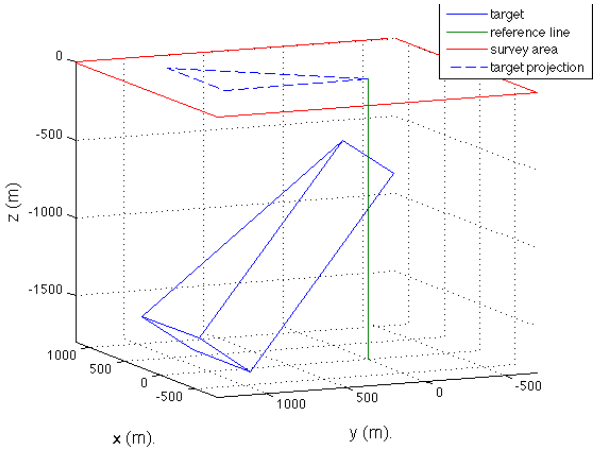

Figure 2: Triangular prismatic test target of thickness 400m.

This test target was subjected to anomaly calculations for various target distances, for the vertex, line, surface methods and the new volume method. Figure 3 shows an initial downward trend, indicating the expected approach to the point source with increasing target distance. However, at about 10^3 target diameters, the vertex method errors have grown to equal the difference from the point source, and at greater target distances the effective deviation from the point source now increases. At about $10^{3.9}$ target diameters, a similar divergence from the point source anomaly occurs for the line method, and at about $10^{5.2}$, for the surface method. Finally, the new volume method approaches the point source until about 10^8 target diameters, after which the relative difference becomes the minimum possible, about ε, and remains so without growth throughout the remaining synthetic survey test to 10^{16} target diameters. The observed integer error slopes from 3 down to 0 for the four methods is anticipated from the theory given above for the growth factors of γ^{-3} to γ^0 for the four methods. In particular, the aimed for stability of the new method has been demonstrated.

DISCUSSION AND CONCLUSIONS

Improved stability methods in the sequence of vertex, line and surface methods for polyhedral gravi-magnetic anomalies have been known for some years, but the formulation of a zero error growth method has not been achieved previously. A difficulty has been the appearance in the anomaly formulae of the absolute value of the normal projection $|v_i|$ of the vertex position vectors on the i facets. Even though the target distance may be large, the value of v_i may be small and of either sign, depending on whether the observation point is just above or below facet i. Differencing over terms $|v_i|$ to devise offsets for cancelling dominant terms therefore could not be devised. The matter was resolved here by first constructing zero-growth anomaly formulae for the polygonal sheet anomaly. The dominant term there has to be the equivalent point source term,

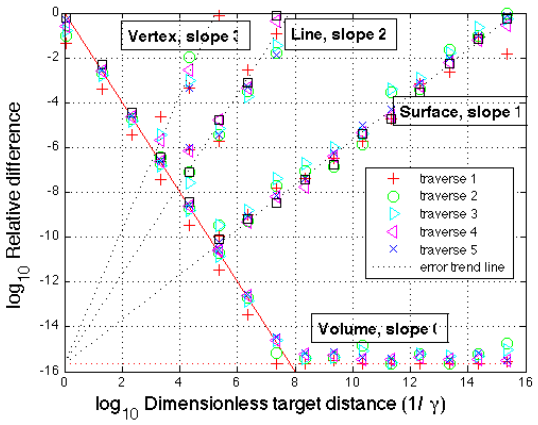

Figure 3: Error plots for Vertex, Line, Surface and Volume methods.

located at the sheet centroid. The centroid has the same vertical projection as any of the sheet's vertex position vectors, and so the problem of differencing across near but unequal values of $|v|$ does not arise. The key insight was to view the polyhedral anomaly as a sum of facet-sheet anomalies, and to exploit gravi-magnetic similarity for treating sheet and polyhedral anomalies in the same framework.

The extra arithmetic complexity of the volume method means that it will not replace the simpler but less stable line method. However, the present work is likely to find application in the construction of reliable modelling software, forming a benchmark for testing algorithms that do not use the stabilized forms. This is particularly important when single precision has to be used, or where large target distance to target sizes occur, such as in whole earth modelling, or using models with very fine triangulations that have been generated by a visual renderer.

The work presented here demonstrates the construction of a stable polyhedral magnetic anomaly formula. On account of gravi-magnetic similarity, stable algorithms can be found for all the standard gravi-magnetic anomalies of uniform polyhedral targets.

APPENDIX A

DETAILED FORMULAE

The functions Atnh, Atn respectively can be computed in a stable way from their Taylor series expansions

$$\begin{aligned} \text{Atnh}\, x &= 1/3! + x^2/5! + x^4/7! + \ \ldots\ , \\ \text{Atn}\, x &= -1/3! + x^2/5! - x^4/7! + \ \ldots\ . \end{aligned} \tag{A-1}$$

Surface and volume methods will in practice be used at large distances from the target, with small arguments x, and so require only a few terms of the series to be evaluated.

Differences $\delta\Lambda_j = \Lambda_j - \Lambda_j^*$, $\delta\lambda_j = \lambda_j - \lambda_j^*$ are computed as stabilized $O(\gamma^2)$ quantities from

$$\begin{aligned} \delta\Lambda_j &= \Lambda_j\bar{\Delta}_j\ , && \text{(A-2)} \\ \delta\lambda_j &= (\lambda_j+\tilde{\lambda}_j)\bar{\Delta}_j + \tilde{\lambda}_j\Lambda_j\Lambda_j^*\ , && \text{(A-3)} \\ \bar{\Delta}_j &= \tfrac{1}{2}(\Delta_{j1}+\Delta_{j2}), && \text{(A-4)} \\ \tilde{r}_c &= r_c + |v|\ , && \text{(A-5)} \\ \Lambda_j^* &= \mathscr{L}_j/(2r_c), && \text{(A-6)} \\ \lambda_j^* &= h_j\Lambda_j^*/\tilde{r}_c, && \text{(A-7)} \\ \tilde{\lambda}_j &= r_c\ \lambda_j^*/\tilde{r}_j\ , && \text{(A-8)} \\ \Delta_{jk} &= (\frac{\mathbf{R}_c-\mathbf{R}_{jk}}{r_c})\cdot(\frac{\mathbf{r}_c+\mathbf{r}_{jk}}{r_c+r_{jk}}),\ k=1,2\ . && \text{(A-9)} \end{aligned}$$

The starred notation indicates that $O(\delta)$ j-subscripted quantities have been replaced by centroid-related quantities r_c or $\mathbf{r}_c$.

APPENDIX B

STABILIZED SECOND ORDER DIFFERENCES

Differences (15) are to be stablized to $O(\gamma^3)$ by

$$\begin{aligned} \delta^2\Lambda_j &= \tfrac{1}{2}(\Lambda_j+\Lambda_j^*)\delta\bar{\Delta}_j + \tfrac{1}{2}\delta\Lambda_j(\bar{\Delta}_j+\bar{\Delta}_j^*) && \text{(B-1)} \\ \delta^2\lambda_j &= \tfrac{1}{2}(\delta\lambda_j+\delta\tilde{\lambda}_j)(\bar{\Delta}_j+\bar{\Delta}_j^*) + \tfrac{1}{2}(\lambda_j+\lambda_j^*+\tilde{\lambda}_j+\tilde{\lambda}_j^*)\delta\bar{\Delta}_j + \\ &\quad \tilde{\lambda}_j\Lambda_j\Lambda_j^* && \text{(B-2)} \end{aligned}$$

where

$$\begin{aligned} \delta\bar{\Delta}_j &= \tfrac{1}{2}(\delta\Delta_{j1}+\delta\Delta_{j2}), && \text{(B-3)} \\ \delta\Delta_{jk} &= -\tfrac{1}{2}\left((\mathbf{R}_c-\mathbf{R}_{jk})/r_c\right)^2 + \tfrac{1}{2}\Delta_{jk}^2 && \text{(B-4)} \\ \bar{\Delta}_j^* &= (\mathbf{R}_c-\bar{\mathbf{R}}_j)\cdot\mathbf{r}_c/r_c^2, && \text{(B-5)} \\ \delta\Lambda_j^* &= \Lambda_j^*\bar{\Delta}_j^*, && \text{(B-6)} \\ \tilde{\lambda}_j^* &= \lambda_j^* r_c/\tilde{r}_c, && \text{(B-7)} \\ \delta\lambda_j^* &= (\lambda_j^*+\tilde{\lambda}_j^*)\bar{\Delta}_j^*, && \text{(B-8)} \\ \delta\tilde{\lambda}_j &= \tilde{\lambda}_j^*(\bar{\Delta}_j r_c + \Lambda_j^2\tilde{r}_j)/\tilde{r}_j\ . && \text{(B-9)} \end{aligned}$$

APPENDIX C

SHEET CENTROID OFFSET

$$\begin{aligned} <\mathbf{r}_{ic},\mathbf{r}_p> &= \frac{\mathbf{r}_{ic}}{r_{ic}^3} - \frac{\mathbf{r}_p}{r_p^3} \\ &= \tfrac{1}{2}(\mathbf{r}_{ic}-\mathbf{r}_p)(\frac{1}{r_{ic}^3}+\frac{1}{r_p^3}) + \tfrac{1}{2}(\mathbf{r}_{ic}+\mathbf{r}_p)(\frac{1}{r_{ic}^3}-\frac{1}{r_p^3}) \\ &= \tfrac{1}{2}(\mathbf{R}_{ic}-\mathbf{R}_p)(\frac{1}{r_{ic}^3}+\frac{1}{r_p^3}) - \tfrac{1}{2}(\mathbf{r}_{ic}+\mathbf{r}_p)\frac{\delta r_{icp}}{r_{ic}r_p} \\ &\quad \times(\frac{1}{r_{ic}^2}+\frac{1}{r_{ic}r_p}+\frac{1}{r_p^2})\ , && \text{(C-1)} \\ \delta r_{icp} &= r_{ic}-r_p \\ &= (\mathbf{R}_{ic}-\mathbf{R}_p)\cdot(\frac{\mathbf{r}_{ic}+\mathbf{r}_p}{r_p+r_{ic}})\ . && \text{(C-2)} \end{aligned}$$

The final versions of equations (C-1) and (C-2) are to be used in computations.

REFERENCES

Holstein, H., 2002, Gravimagnetic similarity in anomaly formulas for uniform polyhedra: Geophysics, **67**, 157–167.

Holstein, H., and C. Anastasiades, 2010a, Asymptotic anomalies of uniform thin polygonal sheets: Presented at the EAGE, 4th International Conference and Exhibition, St Petersburg.

———, 2010b, Finitely expanded gravity anomaly of uniform thin polyhedral sheets: Presented at the 72nd EAGE Conference and Exhibition, Barcelona.

Holstein, H., D. Fitzgerald, and C. Anastasiades, 2009, Gravimagnetic anomalies of uniform thin polygonal sheets: Presented at the 11th biennial meeting and exhibition, South African Geophysical Association.

Holstein, H., P. Schürholz, A. Starr, and M. Chakraborty, 1999, Comparison of gravimetric formulas for uniform polyhedra: Geophysics, **64**, 1438–1446.

Strakhov, V., M. Lapina, and A. Yefimov, 1986, A solution to forward problems in gravity and magnetism with new analytical expressions for the field elements of standard approximating bodies I: Izvestiya, Earth sciences, **22**, 471–482.